Innovative Infrastructure Solutions (2022) 7:159
https://doi.org/10.1007/s41062-022-00758-3

TECHNICAL PAPER

Reliability assessment of a marine bridge structure considering Indian climatic conditions under time-variant loads

Mukunda Madhab Borah[1] · **Abhijeet Dey**[1] · **Arjun Sil**[1]

Received: 18 November 2021 / Accepted: 25 January 2022 / Published online: 21 February 2022

Abstract

Environmental factors have an impact on the efficiency, serviceability, and stability of reinforced concrete (RC) structures. Chloride-induced corrosion has now been recognized as a major cause in the degradation of RC structures service life. This paper introduces a model for conducting time-variant reliability analysis of corrosion-affected bridges in India's coastal region. The current study presents a multi-hazard approach for assessing the time-dependent reliability of RC bridges, taking into account chloride-induced corrosion hazard, time-dependent non-stationarities in load and strength, and climate change related to seasonal variation. The research was carried out using an advanced corrosion rate model that captured nonlinear behaviour, necessitating pitting corrosion as a realistic corrosion degradation process rather than uniform corrosion. Until now, most studies on corrosion deterioration of RC bridges assumed a static or time-varying degradation process that was unaffected by in situ climate conditions. The impact of climatic conditions, notably temperature and relative humidity, on the corrosion degrading process was underlined in this study. The framework demonstrates that anticipated changes in climatic factors are likely to exacerbate the failure probability of corrosion-affected bridge structures when applied to a conventional T-girder bridge (named Sardar Bridge) in Surat district of Gujarat (India). The findings emphasize the need of taking environmental parameters like temperature and relative humidity into account when analysing the reliability of RC bridges that have been subjected to chloride-induced deterioration.

Keywords Climate · Corrosion · In situ · Reliability · Time variant

Introduction

The operational safety along with serviceability of reinforced concrete structures during their service life depends on several external as well as internal factors. External factors include the operational as well as environmental considerations. The deterioration of structures due to dead loads, live loads and other loads is called operational degradation, whereas the environmental degradation is caused by the conditions of the surrounding environment the structure is subjected to, such as the temperature, relative humidity, chloride concentration, and carbonation. The operational and environmental factors together have an effect on the deterioration of reinforced concrete structure. The reinforced concrete structures are prone to corrosion when exposed to environments containing high chloride concentration [10, 26]. The chloride-induced corrosion is one of the main driving mechanisms of deterioration of RC structures. Previous literatures [14, 35] on corrosion modelling have developed reliability models by taking into consideration the time-variant parameters of chloride-induced corrosion mechanism, and some research [36, 27] has considered both spatial and temporal variables for reliability analysis. On the other hand, [3] conducted reliability analysis with coupled effect of corrosion with fatigue or with biodeterioration [2]. Also, multiple studies [1, 30] have been conducted to find out the influence of environmental parameters on the corrosion process. In spite of that, studies on reliability that focusses on the impact of environmental and climatic factors like temperature and relative humidity on the corrosion process are rare. Numerous work [6, 9, 17] done on chloride-induced corrosion mechanism have overlooked the in situ temperature and relative humidity condition which may vary from the reference laboratory condition in determining the corrosion rate. Because chloride-induced

✉ Mukunda Madhab Borah
mailto.mukundamadhab@gmail.com

[1] Dept of Civil Engineering, NIT Silchar, Silchar, Assam 788010, India

corrosion is treated as an electrochemical thermodynamic mechanism, corrosion rate is influenced by temperature [21, 22] and humidity [23] that might undergo changes due to seasonal changes. A study conducted by [37, 40] revealed that on rise in temperature by 2 °C results in 15% increase in chloride corrosion rate. Bastidas-Arteaga et al., (2013) developed a probabilistic approach to determine the lifetime of structure subjected to chloride ingress taking into consideration the effect of climate change due to global warming which revealed around one third reduction in service life due to elevated temperature. The findings of [31] indicate that a changing climate could increase the level of damage to reinforced concrete infrastructure by up to 6%. [40] discovered that the spatiotemporal impact of a changing climate would increase current estimates of carbonation-induced damages by over 16% in Australia 29. [11] found that variation of temperature and relative humidity over a 100-year period were found to be liable for a reduction in service life from 7.8 to 10.2 years. Similarly, several researchers have highlighted on the importance of considering the influence of temperature change due to climate change on corrosion rate [4, 5, 8, 19, 31, 39–41]. Despite this, there is minimal work available that have been attentive in incorporating the in situ temporal and spatial variation of climatic factors like temperature and relative humidity across the world into reliability assessment framework.

In this paper, the choice of the Indian coastal region as a research area makes a fresh addition to the broad domain of reliability assessment of corrosion-affected bridges. As India shares a 7500-km-long coastline with the Arabian Sea, Indian Ocean, and Bay of Bengal, the study area is relevant because of the region's high chloride-laden environment. In previous work by the author [6], the salinity of the water around the Indian subcontinent was researched and mapped as shown in Fig. 1 to provide a basic concept of the quantity of chloride to be encountered in case of marine structures.

Due to the high concentration of chloride in Indian coastal region, the reliability of a conventional T-girder bridge (named Sardar Bridge) in Surat district of Gujarat (India) was examined in this study. Bridges are a critical component of a nation's infrastructure [7]. Gujrat, a coastal region in India, has a high concentration of chloride. As a result, the RC bridge structures in this region, which serves as a vital transportation corridor, are irreparably harmed by reinforcement corrosion. The malfunctioning of such bridges impedes the socioeconomic development of that area by hindering significant traffic flow/volume. The average traffic volume on Gujarat's bridges is 13,000 passenger car units (PCU) per hour, which might be called heavy traffic condition [13]. Keeping that in mind, the authors [13] undertook a study by taking into account the vast volume of live load encountered by an RC bridge over its lifetime and also considering the time-dependent arbitrary character of

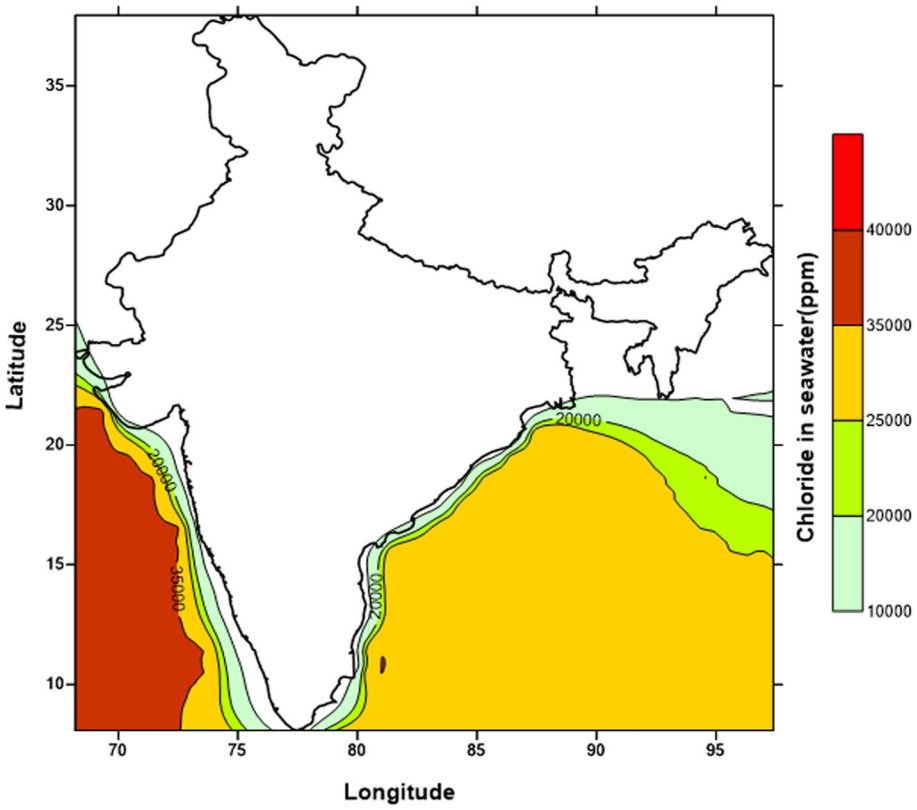

Fig. 1 Salinity of Seas surrounding India [6]

both structural loads and strength. The study also took into account several environmental factors such as alkali–silica reaction, corrosion, sulphate assault, and freeze-thaw. The research was effective in projecting the lifetime of degrading RC bridges, as well as determining the best time for condition monitoring and developing maintenance measures to ensure the bridges continuing service life. This study, on the other hand, attempts to fulfil the research gap in previous work by proposing a multi-hazard reliability assessment framework for highway RC bridges that takes into account the influence of structural loads, structural deterioration due to chloride-induced corrosion, and the effect of climatic factors such as temperature and relative humidity. This research looks into the effects of changes in temperature, relative humidity, and chloride concentration on the corrosion deterioration process over the course of a lifetime. The current work is an extended version of the authors' previous work [13], as the model for determining the failure probability of structures under chloride attack is diversified to explicitly incorporate the implications of probable seasonal changes in temperature and relative humidity of a region. The complex interplay of these two key variables (Temperature and Relative Humidity) as a measure of seasonal change are investigated for four different seasons: 1. Winter (December–Feb) 2. Summer (March–May) 3. Monsoon (June–September) 4. Post-Monsoon (October–November).

Another novelty aspect of this research is the use of an advanced corrosion rate model to estimate structural reliability, which is a better version of the traditional corrosion rate models offered by several country codes such as Duracrete and CECS. One of the authors established this model in a recent study on fragility [12]. The most significant advancement in the advanced corrosion rate model is that it replaces the rapid or abrupt increase in corrosion rate at the commencement of early concrete cracks with a steady propagation phase, so as to capture the nonlinearity (increasing trend in intermediate phase and thereafter decreasing) after the initial cracking of the concrete. Current available literature examining the effect of chloride-induced corrosion on the reliability of deteriorating highway bridges use solely a linear corrosion rate model, overlooking the nonlinear pattern that occurs during the entire period. Because nonlinearity in corrosion propagation has a stronger harmful effect than linear corrosion propagation, under actual field conditions, such oversimplified assumptions may contribute to an underestimation of the reliability of bridges. Unlike previous research, which assumed that reinforcement degradation due to chloride ingress was uniform, the results derived from using the advanced corrosion model provide a more realistic and intriguing picture of the actual deterioration process as per basic corrosion mechanism.

Variation of climatic conditions in India with seasons

The climatic condition of India encompasses an extensive range of weather conditions owing to its huge geographical extent and diverse topography. The climate of India can be generally defined as tropical monsoon type. The Indian Meteorological Department (IMD) has classified Indian climate into four seasons: 1. Winter (December–Feb) 2. Summer (March–May) 3. Monsoon (June–September) 4. Post-Monsoon (October–November). Due to the vast size of India, the climatic pattern is also significantly affected. For instance, the regions in the proximity of sea experience marine climate, while the regions far from sea experience a continental-type climate. The areas to the south of tropic of cancer exhibit tropical climate, while the areas to the north of tropic of cancer experiences warm temperate climate. Therefore, there occurs both spatial and temporal variation of climatic factors. This calls for a need to study the variation of temperature and relative humidity across India with respect to location and time. Due to the vastness of the country, the temperature differs from region to region. A time series data of average values of minimum, maximum, and average temperature across India over 40 years span are shown in Fig. 2a. The trend shows the variability of temperature with respect to time and also the gap between average maximum and average minimum temperature in a year. Similarly, Fig. 2b shows the time-series variation of average relative humidity across India in past 40 years. Therefore, it is necessary to incorporate the timely variation of temperature and relative humidity of a region in reliability analysis. Figure 3 exhibits the spatial variation of temperature and relative humidity across India in summer and winter season. From the figure it is clearly evident that the temperature and humidity of a place varies with change of seasons. Hence, the seasonal variation of temperature and relative humidity of a region will also exert a major influence on chloride-induced corrosion mechanism and should be properly looked into.

This article is structured as follows. The next segment explores the role of temperature and relative humidity on the corrosion process caused by chloride. The effect of changes in climatic factors such as temperature and relative humidity on the governing equations that predict corrosion initiation time and rate is addressed. A new modified equation for corrosion initiation time is put forward. The mathematical modelling of an RC bridge affected by chloride ingress by taking in consideration of in situ climatic conditions is the subject of the next section. This paper presents representative T-girder RC bridge (Sardar Bridge) located in Gujarat as the case-study structure type to explore the impact of chloride exposure conditions and seasonal climate variation along with time-variant and independent live load models on

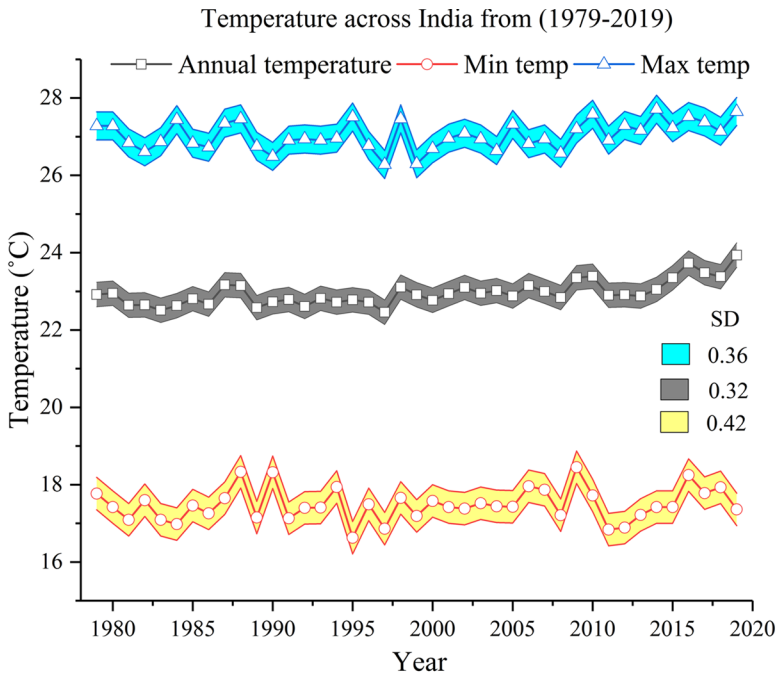

(a) The average annual, maximum and minimum temperature of India (1979-2019) [NOAA]

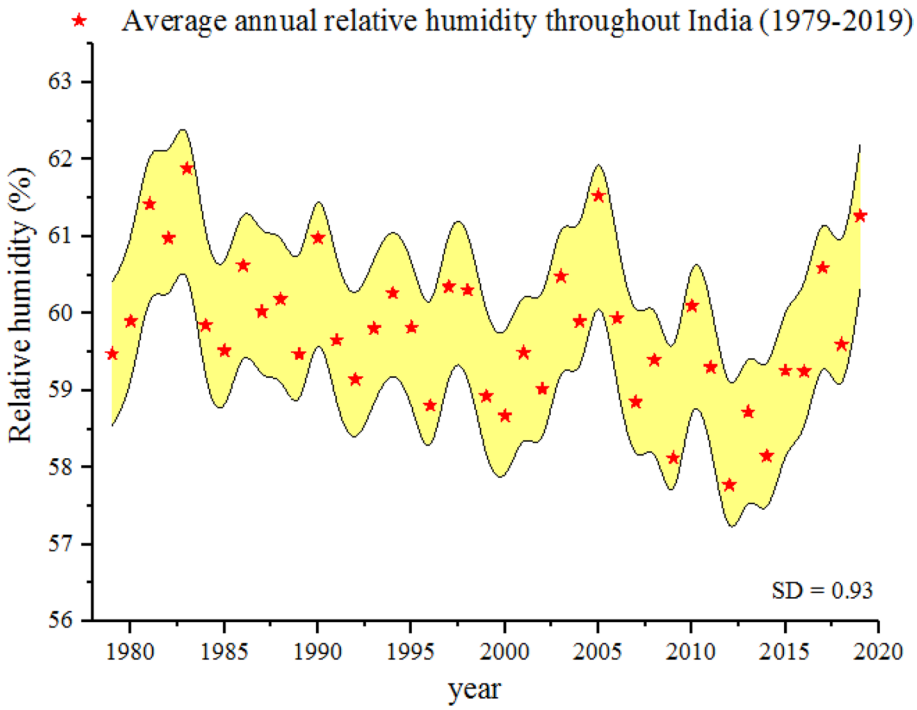

(b) The average annual relative humidity of India (1979-2019) [NOAA]

Fig. 2 **a** Average annual, maximum and minimum temperature of India (1979–2019) [NOAA]. **b** Average annual relative humidity of India (1979–2019) [NOAA]

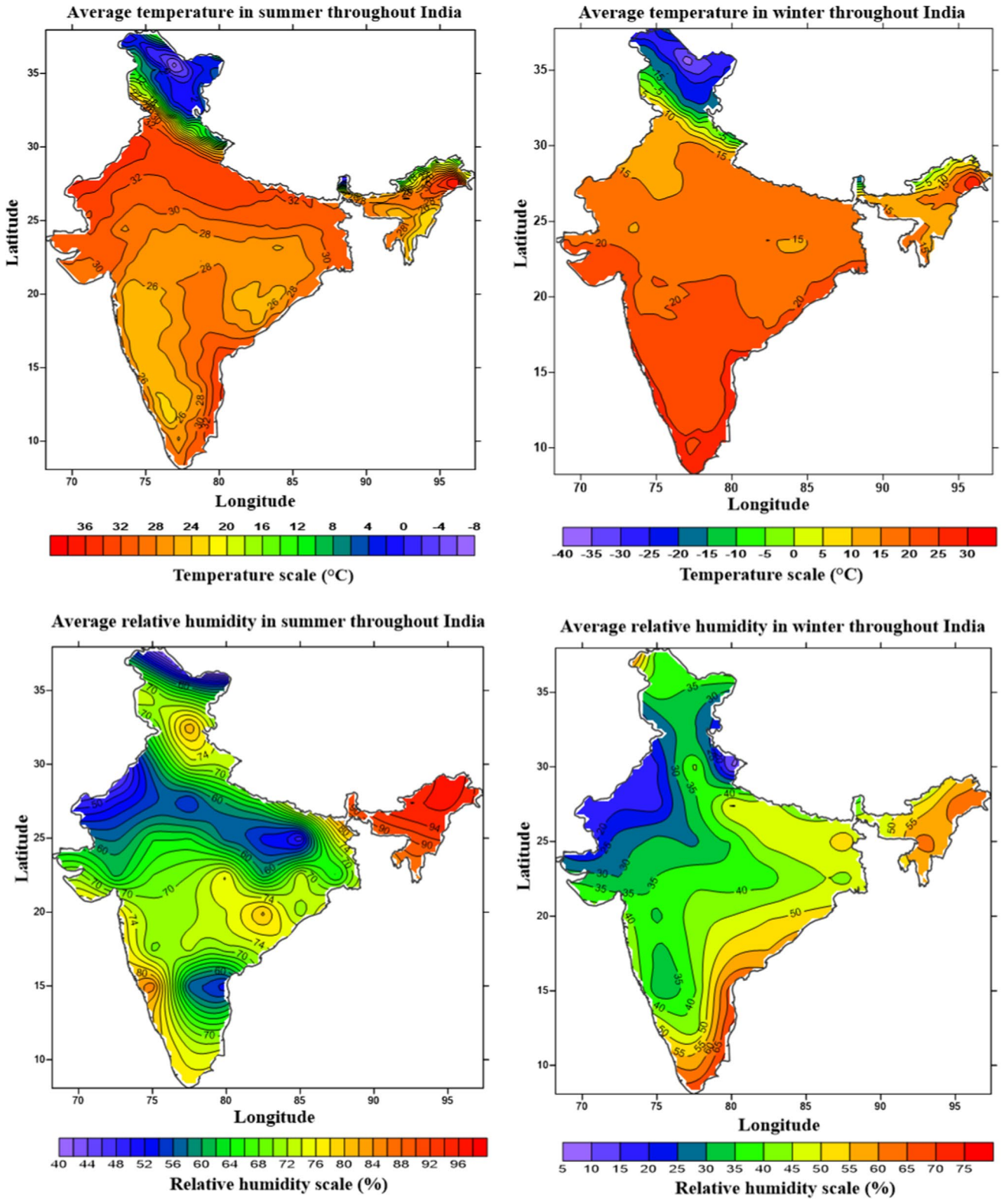

Fig. 3 Temperature and humidity variation throughout India [NOAA]

the reliability of the structure. The paper ends with conclusions and recommendations for future work.

Chloride-induced corrosion considering temperature and relative humidity variation

Chloride-induced corrosion of RC structure remains one of the most prominent reasons of structural deterioration of RC bridges. Corrosion is primarily caused due to ingress of chloride when structures are subjected to a chloride-contaminated environment in combination with insufficient concrete cover and inferior quality of concrete. Deterioration of concrete structures due to corrosion consists to two stages. First is the corrosion initiation stage, i.e. time till commencement of corrosion in reinforcement and secondly propagation stage. The subsequent topics of discussion briefly present the basic models that have widely been used in research to model the chloride-induced degradation together with variations in model parameters to demonstrate the effect of temperature and relative humidity in chloride-induced corrosion mechanism.

Corrosion initiation time

The corrosion initiation time corresponds to the time required for chloride ions to diffuse into concrete through concrete cover and activate corrosion in the steel concrete interface. Corrosion initiates when the concentration of chloride exceeds a critical value or threshold value of chloride concentration at reinforcement surface. Several researchers have put forwarded and implemented existing models to calculate initiation time of chloride-induced corrosion. One such widely used model is recommended by [15] which is used by the authors in their previous work to calculate corrosion initiation time for structure subjected to marine environment [6].

$$t_{\text{ini}} = X_1 \left[\frac{C_{\text{v}}^2}{4 n_{\text{e}} n_{\text{t}} n_{\text{c}} D_0 (t_0)^r} \left[\text{erf}^{-1}\left(1 - \frac{C_{\text{cr}}}{C_{\text{s}}}\right)\right]^{-2} \right]^{\frac{1}{(1-r)}} \quad (1)$$

where t_{ini} = corrosion initiation time (t_i) (years), C_{v} = concrete cover (mm), D_0 = Diffusion coefficient at time t_0 (mm^2/s), t_0 = reference period (28 days), C_{s} = surface chloride content (kg/m^3 or % of binder) = $A_c(w/c)$, C_{cr} = critical or threshold chloride content (kg/m^3 or % of binder), n_{e} = environmental factor, n_{t} = test factor for empirical diffusion coefficient determination, n_{c} = factor for curing time correction, r = ageing factor, X_1 = model uncertainty to account for variation in input parameters and idealization implied by Fick's second law. All the parameters used in Eq. (1) are summarized in Table 1.

Table 1 Variables used to predict the corrosion initiation time [6]

Parameter	Condition	Units	Distribution	Mean	Variance
n_e	All submerged/ tidal/ splash/ atmospheric	–	Normal	1	0.09
n_t	All	–	Normal	0.85	0.09
n_c	All	–	Normal	0.8	0.01
r	All	–	Normal	0.25	0.05
A_c	Submerged	–	Normal	10.35	0.50
	Tidal		Normal	7.74	0.80
	Splash		Normal	7.74	0.80
	Atmospheric (0 km from seashore)		Normal	6.44	0.78
X_1	All	–	Lognormal	1	0.006

While the aforementioned equation has been successfully implemented by researchers to calculate the corrosion initiation for RC bridge structures subjected to marine environment throughout various locations, the effect of climatic factors like temperature and humidity of the location on the corrosion process is not considered. Duracrete model adopts as 20 °C and 75% as reference values of temperature and relative humidity, respectively. Therefore, any deviation from reference values would either lead to underestimation or overestimation of corrosion initiation time in locations where there is a variation of in situ temperature and relative humidity form their reference values. To address this problem, the influence of temperature and relative humidity must be included to model the chloride-induced corrosion process. In this context, the mathematical model implemented by El-Hassan et al. [19] and Martin-Perez et al. [28] facilitates in assessment of coefficient of diffusion for chloride ingress at a certain temperature and relative humidity level as follows:

$$D_0(T, \text{RH}) = D_{0,\text{ref}} \times F_1(T) \times F_2(\text{RH}) \quad (2)$$

where reference diffusion coefficient is $D_{0,\text{ref}} = 10^{(-12.06+2.4w/c)} (m^2/s)$ [6, 38].

$F_1(T)$ and $F_2(\text{RH})$ = adjustment functions for temperature and humidity, given by

$$F_1(T) = e^{\left[\frac{U}{R}\left(\frac{1}{T_{\text{ref}}} - \frac{1}{273+T}\right)\right]}$$

$$F_2(\text{RH}) = e^{\left[1 + \frac{(1-\text{RH})^4}{(1-\text{RH}_{\text{ref}})^4}\right]^{-1}}$$

where U = activation energy of chloride diffusion process (kJ/mol), R = gas constant (8.314 J mol^{-1} K^{-1}), T_{ref} and RH_{ref} = Reference values, 293 K or (20 °C) for temperature and (75%) for relative humidity, T(°C) = in situ temperature, and RH = in situ value of relative humidity.

Time-dependent variation of diffusion coefficient is obtained as: [29].

$$D(t) = D_0(T, \mathrm{RH}) \times \left(\frac{t_{\mathrm{ref}}}{t}\right)^m \tag{3}$$

where D(t) = diffusion time at time t, t_{ref} = 28 days and m = decay constant or age factor = 0.37 [6].

On implementation of the impact of on field temperature and relative humidity, the modified corrosion initiation equation is shown as follows:

$$t_{\mathrm{ini}} = X_1 \left[\frac{C_{\mathrm{v}}^2}{4 n_{\mathrm{e}} n_{\mathrm{t}} n_{\mathrm{c}} D_0(T, \mathrm{RH})(t_0)^r}\left[erf^{-1}\left(1 - \frac{C_{\mathrm{cr}}}{C_{\mathrm{s}}}\right)\right]^{-2}\right]^{\frac{1}{(1-r)}} \tag{4}$$

To illustrate the influence of temperature and relative humidity on diffusion coefficient, let us consider an example from previous work. The concrete is assumed to be prepared of OPC with a water cement ratio of 0.4 [6]. The reference diffusion coefficient $D_{0,ref}$ is adopted from previous work [6]. To demonstrate the influence of temperature and relative humidity on diffusion coefficient, three different temperatures and relative humidity levels are considered. Both the parameter values have been considered by keeping in mind the temperature and relative humidity condition across the year in National capital city Delhi. Figure 4a, b shows the annual variation of temperature and relative humidity in Delhi. Three temperatures and relative humidity values are adopted to capture the variation throughout different time of year, i.e. T_{min} = 10 °C; T_{avg} = 33 °C; T_{max} = 45 °C; RH_{min} = 35%; RH_{avg} = 50%; RH_{max} = 80%.

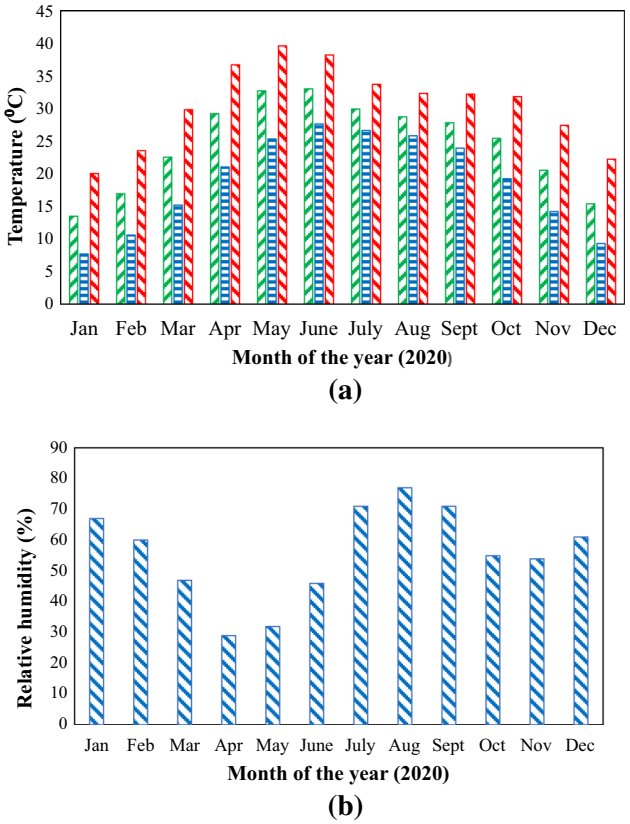

Fig. 4 Month-wise variation of (**a**) temperature and (**b**) relative humidity of Delhi https://en.climate-data.org/

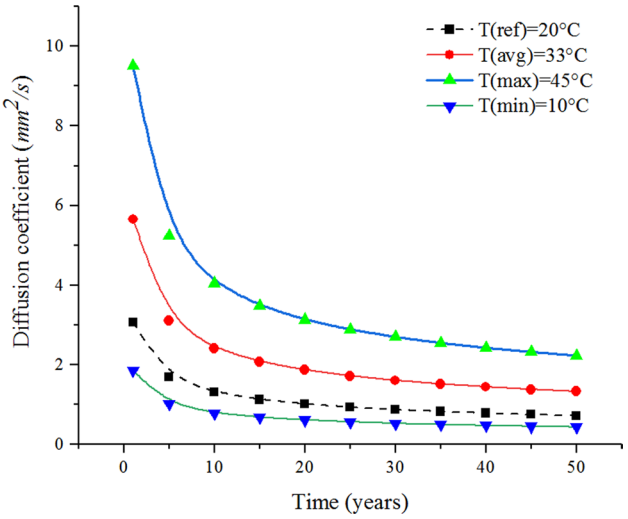

Fig. 5 Diffusion coefficient progression with time considering RH_{ref} = 75%

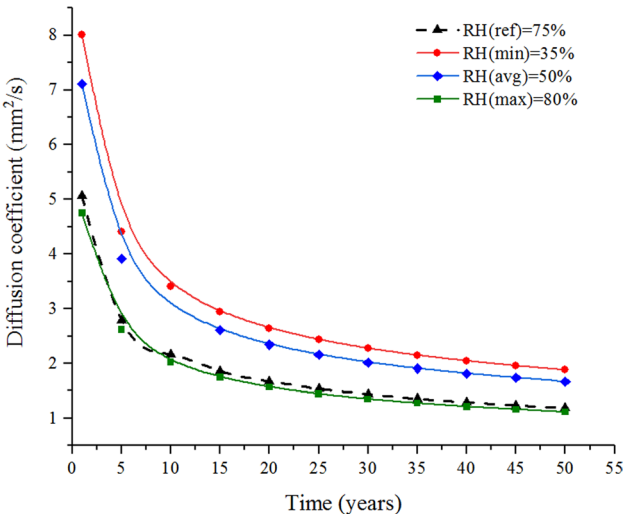

Fig. 6 Diffusion coefficient progression with time considering T_{ref} = 20 °C

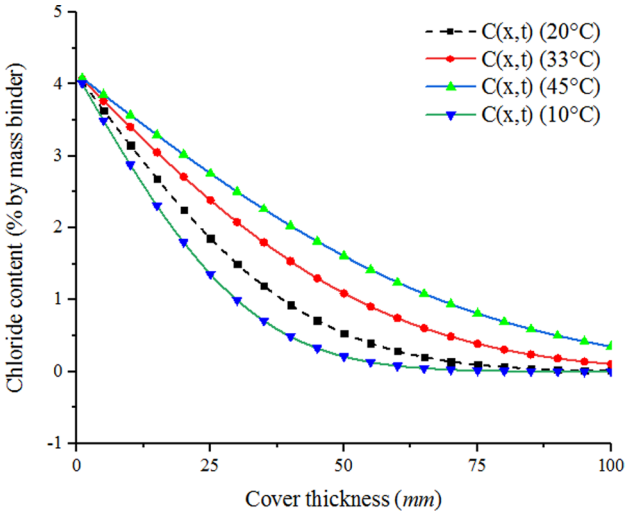

Fig. 7 Chloride ingress profile at varying temperature and constant RH = 75%

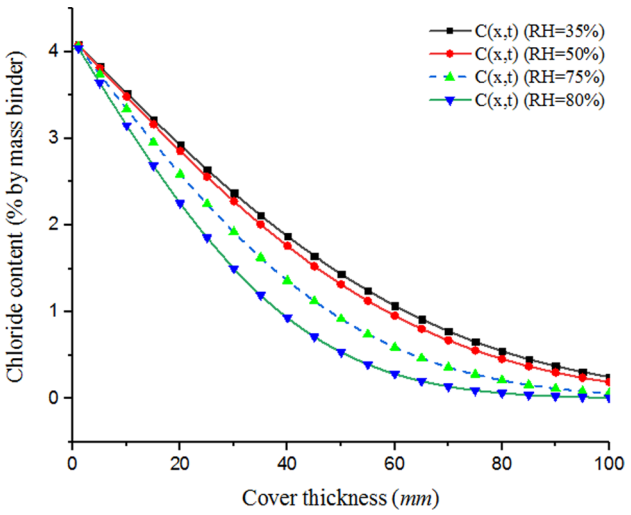

Fig. 8 Chloride ingress profile at varying temperature and constant $T = 20$ °C

Figure 5 shows the change of diffusion coefficient over time for different temperatures while considering the relative humidity constant as 75% for each case. It is observed that with the rise of temperature, the diffusion coefficient values are higher. But from Fig. 6, an opposite trend is observed, i.e. the diffusion coefficient values are lower for higher value of relative humidity. Therefore, it can be inferred that the diffusion coefficient is directly proportional to temperature and inversely proportional to relative humidity. Therefore, both temperature and humidity together will play a critical role in determining the corrosion initiation time.

Similar observations are also made from Figs. 7 and 8 for chloride ingress profile after 5 years while considering surface chloride concentration as $C_s = 4.14\%$ (by mass of binder) [6].

Dependence of corrosion rate on temperature and humidity

After initiation of corrosion, the propagation stage follows, which leads to loss of cross-sectional area of reinforcement due to accumulation of corrosion products along with other effects like cracking and spalling of concrete cover. The propagation stage is the time needed for corrosion to propagate to such a degree that the load carrying capability of the structural member becomes inadequate. While the preceding section showcased the importance of including the in situ temperature and relative humidity to determine corrosion initiation time, in this segment, emphasis is given on the effect of temperature and relative humidity on the propagation stage. The rate at which corrosion propagates resulting in loss of cross-sectional area of rebar is calculated with the help of corrosion current density (i_{corr}). Based on previous literature on corrosion rate measurement, Vu and Stewart [35] proposed a model for calculation of corrosion current density (i_{corr}) considering a constant reference temperature and relative humidity level of 20 °C and 75%, respectively. The corrosion current density is influenced by the availability of water and oxygen at the surface of steel, and can therefore be modelled as a function of water cement ratio (w/c) and cover thickness C_v. The corrosion current density can be expressed as [35]:

$$i_{corr,0} = \frac{37.8(1 - w/c)^{-1.64}}{C_v}\left(\mu A/cm^2\right) \tag{5}$$

Significant research has described corrosion rate as a time-dependent variable which decreases throughout the life of the structure. The decrease in corrosion rate over time can be justified by the fact that as corrosion progresses, the corrosion products accumulate in the reinforcement surface which makes oxygen and moisture harder to reach the steel surface [15, 18, 24].

To calculate the time-varying corrosion rate, Liu and Weyers [24] and Vu and Stewart [35] proposed an empirical equation based on numerous experimental data as:

$$\lambda = \frac{dp}{dt} = 0.0116 \times i_{corr,0} \times 0.85\left(t - t_{ini}\right)^{-0.29} \tag{6}$$

Even though this equation has been widely used to calculate reliability of RC structures subjected to chloride-induced corrosion, [16, 32–34] the effects of temperature and humidity variation is ignored.

In this work, an advanced corrosion rate model is utilized to calculate the reliability of RC bridges instead of the traditional corrosion rate model. The advanced corrosion rate

model has been divided into three phases, each of which corresponds to the actual corrosion process. The process of chloride-induced corrosion is divided into three stages. The first stage covers the period from initiation of corrosion to concrete cracking. The corrosion rate in the first stage is expressed in the form of λ_1. At the onset of the second stage, there is a continuous increase in corrosion rate due to commencement of cracking in concrete. This stage would continue all the way through the period of severe cracking of concrete. The quantitative estimation of this stage is reported in very few studies; therefore, in this stage, the corrosion rate is adopted as linearly increasing with time. At this stage, the corrosion rate is assumed to increase linearly with time and is denoted by λ_2. The final stage shows the corrosion rate following severe cracking of concrete and is denoted by λ_3.

To sum up, the model for corrosion rate is summarized as follows [12]:

$$\frac{dp}{dt} = \lambda(t) = \begin{cases} \lambda_1(t) = 0.0116 \times i_{corr,0} \times 0.85\left(t - t_{ini}\right)^{-0.29} & t_{ini} < t \le t_{cr} \\ \lambda_2(t) = (t - t_{cr}) \times \frac{\lambda_3(t_{scr}) - \lambda_1(t_{cr})}{t_{scr} - t_{cr}} + \lambda_1(t_{cr}) & t_{cr} < t \le t_{scr} \\ \lambda_3(t) = (4.5 - 26\lambda_1(t)) \times \lambda_1(t) & t > t_{scr} \end{cases}$$

where t_{ini} = initiation time, t_{cr} = initial cracking time, and t_{scr} = severe cracking time. The advanced corrosion rate model is not explained in details in this paper as it is beyond the scope of this study. However, detailed explanation of advanced corrosion rate model can be found in one of the recent works of the author [12].

To include the effect of climatic factors like temperature and relative humidity on corrosion rate, Guo et al. [18] suggested the addition of two adjustment factors to corrosion current density in Eq. (5). Therefore, the new time-dependent corrosion rate keeping in mind the effect of variation of temperature and relative humidity at time t is given as:

$$i'_{corr,0}(t) = i_{corr,0}(t) \times f_T \times f_{RH}$$

$$\lambda = \frac{dp}{dt} = 0.0116 \times \frac{37.8 \times (1 - w/c)^{-1.64}}{C_v} \times 0.85 \times (t - t_{ini})^{-0.29} \times f_T \times f_{RH} \quad (7)$$

where f_T and f_{RH} are adjustment factors corresponding to temperature (T) and relative humidity (RH). The following section will briefly discuss on the adjustment factors f_T and f_{RH} and will try to incorporate them in the reliability analysis presented in this study.

Adjustment factor f_T to address the effect of temperature.

The effect of variation of temperature on corrosion current density is addressed via adjustment factor f_T in Eq. (6). From previous discussions, it has been observed that in initiation stage, the temperature and relative humidity have substantial effect on the diffusion coefficient, chloride content, and initiation time. Investigations carried out by a number of researchers also point towards a steady decrease in resistivity of concrete on rise in temperature resulting in higher corrosion rates. For example, Stewart et al. [37] noticed a 15% jump in corrosion rate as a consequence of rise in temperature by 2 °C. Duracrete [15] proposed a time-dependent model to estimate corrosion current density at any temperature varying from the reference temperature of 20 °C as shown below:

$i'_{corr}(t) = i_{corr}(t) \times f_T$ where,

$$f_T = \left\{1 + K_T[T(t) - 20]\right\} \quad (8)$$

and $i'_{corr}(t)$ is the corrosion current density at reference temperature and $i'_{corr}(t)$ is the corrosion current density at any temperature. The factor K_T is given by

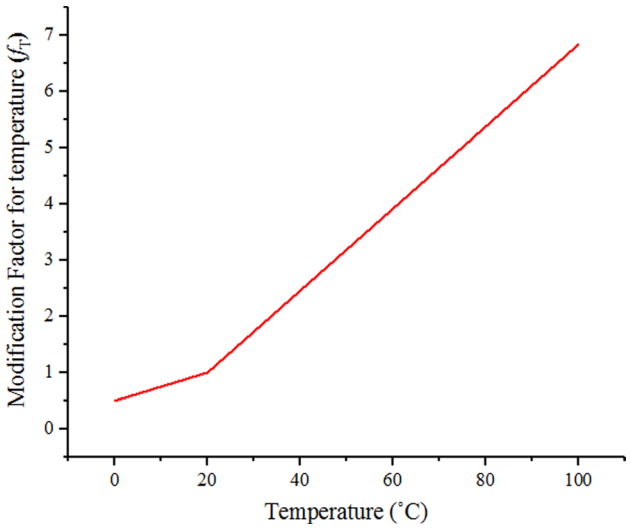

Fig. 9 Adjustment factor for temperature [15]

$$K_T = \begin{pmatrix} 0.025 \ if \rightarrow T(t) \leq 20°C \\ 0.073 \ if \rightarrow T(t) > 20°C \end{pmatrix} \quad (9)$$

Figure 9 shows the variation of f_T with temperature. It is observed that there is a uniform growth of f_T with temperature, but the rate of increase is more when temperature is greater than 20 °C. This indicates that the corrosion rate will increase with an increase in temperature.

Adjustment factor for variation in relative humidity (f_{RH})

The adjustment factor f_{RH} facilitates to evaluate the influence of varying relative humidity on corrosion current density. Grounded on various experimental results, Guo et al. [18] established a theoretical relationship between f_{RH} and relative humidity (RH) as shown below:

$$f_{RH} = e^{-6000\left(\frac{RH-75}{100}\right)^6} \quad (10)$$

The variation of adjustment factor f_{RH} with changing relative humidity can be properly understood from Fig. 10. It is observed that the adjustment factor is noticeably less for RH value lesser than 50% and almost insignificant for RH value less than 35%, whereas as the RH increase from 50 to 65%, there is exponential growth in the value of adjustment factor, and it reaches peak at RH of 85% after which it is observed to be decreasing on subsequent increase in RH above 90% till full saturation is achieved. This is attributed to the fact that when relative humidity reaches saturation, the oxygen cannot reach the surface of reinforcement easily resulting in low corrosion rates.

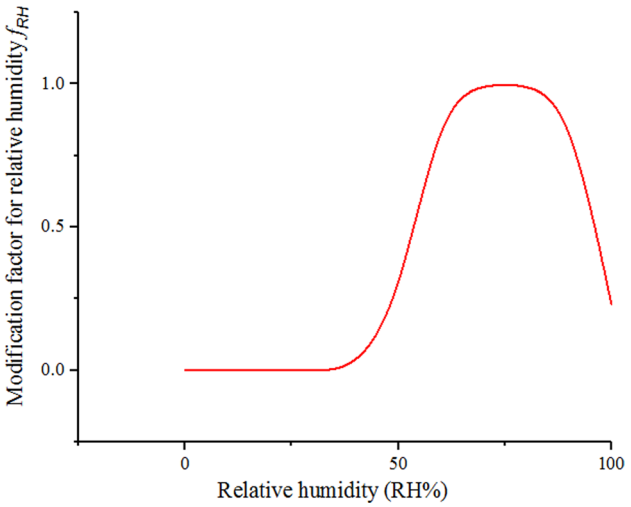

Fig. 10 Adjustment factor for relative humidity [18]

Loss of steel reinforcement area

For reinforced concrete structures, the degradation in strength happens owing to rate of loading applied on the structure, irregularity in properties of material and due to environmental aggressiveness. Corrosion triggered due to ingress of chlorides is one of the foremost causes of degradation of strength of a structure. After attainment of the initiation time of corrosion, the cross-sectional area of steel reinforcement starts to decrease during the course of service life of the structure. The continuous reduction in steel cross-sectional area of reinforcement will lead to a decrease in load carrying capacity of the structure. On implementation of the effect of temperature and relative humidity on corrosion current density, the time-dependent reduction in cross-sectional area of reinforcement can be calculated as [33]:

$$A(t) = \begin{pmatrix} nd_0^2\frac{\pi}{4} \ for & t \leq t_{ini} \\ n[d(t)]^2\frac{\pi}{4} \ for & t_{ini} < t \leq t_{ini} + (d_0/\lambda') \\ 0 \ for & t > t_{ini} + (d_0/\lambda') \end{pmatrix} \quad (11)$$

where d_o = initial diameter (mm); λ = modified corrosion rate; n = number of reinforcement bars. The remaining diameter $d(t)$ of rebar at time T after initiation of corrosion is calculated as:

$$d(t) = d_0 - 0.0232 \int_{t_{ini}}^{T} i'_{corr}(t)dt \quad (12)$$

One commonly used model to express deterioration in strength for aged structures throughout time is given by [25]:

$$R(t) = R_0 \times g(t) \quad (13)$$

where R(t) = Structure's time-dependent strength; R_0 = structure's initial strength; $g(t)$ = function representing the deterioration or degradation of strength = 1-kt and k = rate parameter. Here, g(t) is calculated based on the remaining cross-sectional area of reinforcement after a definite period.

Hazard function with respect to aged structures

The hazard function, $hz(t)$, is defined as the probability of failure of a structure throughout a time interval $(t, t + dt]$ so that it outlives beyond time $(0, t]$ Therefore, the hazard function is mathematically expressed as:

$$hz(t) = -\frac{\mathrm{d}}{\mathrm{d}t} \ln [\mathrm{Rel}(t)] \quad (14)$$

where Rel(t) = Reliability of the structure at time, t

The hazard function $hz(t)$ has a distinctive growth with respect to time throughout structure's deterioration. Upon

Table 2 Design parameters [13]

Sl no	Parameters	
1	Effective span	50 m
2	Clear width of roadway	7.5 m on either side
3	Foot paths	1.25 m wide on either side
4	Thickness of wearing coat	75 mm
5	Spacing of cross girders	5 m c/c
6	Live load	IRC class AA loading
7	Type of construction	Class-I
8	Materials	Deck slab = M-45, PSC 6 girder system = M-50, Wearing coat = M-30, Pile = M-40

attaining the hazard function, the time-dependent structural reliability for structure is stated as:

$$\mathrm{Re}l(t) = \exp\left[-\int_0^t h(\tau)d\tau\right] \tag{15}$$

Structural reliability of chloride-affected bridges

For the survival of a structure at any time *t*, the time-dependent resistance of a structure, R(t), and the effect of load, S(t), should remain in the range of $Z(t) = R(t) - S(t)$. The instantaneous probability of failure $p_f(t)$ during time, t, is therefore expressed as:

$$p_f(t) = p_r[z(t) < 0] = \int_0^\infty F_{\mathrm{R,t}}(x).f_{\mathrm{S,t}}(x)\mathrm{d}x \tag{16}$$

where $F_{\mathrm{R,t}}(x)$ = Instantaneous CDF of structural resistance R, at time t. $f_{\mathrm{S,t}}(x)$ = Instantaneous PDF of load effect S, at time t. It has been assumed that the structural resistance, R, and the effect of load, S, are statistically independent. Therefore, taking into account the occurrence of *n* independent discrete load events, i.e. S_1, S_2,…, S_n, in the span of service life of interval (0, T) and at time periods t_1,t_2,…,t_n, the time-variant probability of failure within (0, T) is mathematically stated as:

$$\mathrm{Re}l(0,T] = P\left[R(t_1) > S_1 \cap R(t_2) > S_2 \cap \ldots\ldots \cap R(t_n) > S_n\right] \tag{17}$$

Fig. 11 Geographic location of Sardar Bridge (Gujarat) [13]

(a)

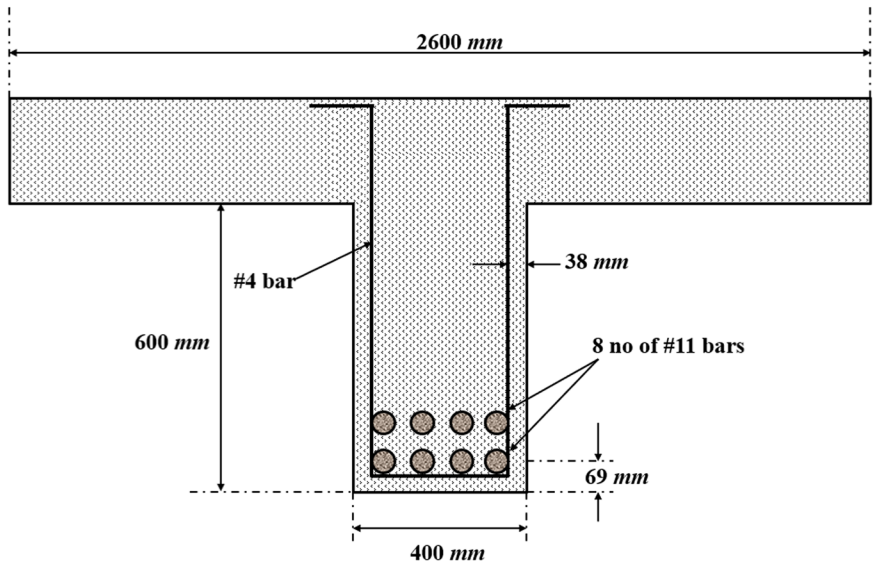

(b)

Fig. 12 **a** Bridge elevation **b** Bridge cross section [13]

Therefore, hazard function, $hz(t)$, at time, t, is stated as:

$$h(t) = \frac{P(T_{\mathrm{f}} \le t + \mathrm{d}t \,|\, T_{\mathrm{f}} > t)}{\mathrm{d}t} = \frac{P(t < T_{\mathrm{f}} \le t + \mathrm{d}t)}{P(T_{\mathrm{f}} > t)\mathrm{d}t} \tag{18}$$

where T_{f} = Random variable representing time of failure.

$P(t < T_{\mathrm{f}} \le t + \mathrm{d}t)$ = Failure probability during time interval $(t, t + \mathrm{d}t)$.

$P(T_{\mathrm{f}} > t)$ = Survival probability up to time, t, of a structural member.

Now, given that the occurrence of load events is considered as a Poisson point process and g(t), R_0 are deterministic, then the probability of failure during the time interval $(t, t + \mathrm{d}t)$ is expressed as:

$$P(t < T_f \le t + dt) = \lambda_r(t)dt \cdot P\left[R_0 \times G(t + dt) < S(t + dt)\right] \cdot P\left[t < T_f\right] \tag{19}$$

By substitution of Eq. (18) in Eq. (17), we can derive that:

$$h(t) = \lambda_r(t)\left[1 - F_s\left(R_0 \times G(t)\right)\right] \tag{20}$$

where $F_s()$ = CDF of load intensity.

$\lambda_r(t)$ = occurrence rate of time-variant mean load.

As a result, the time-variant structural reliability as per Eq. (14) is given by:

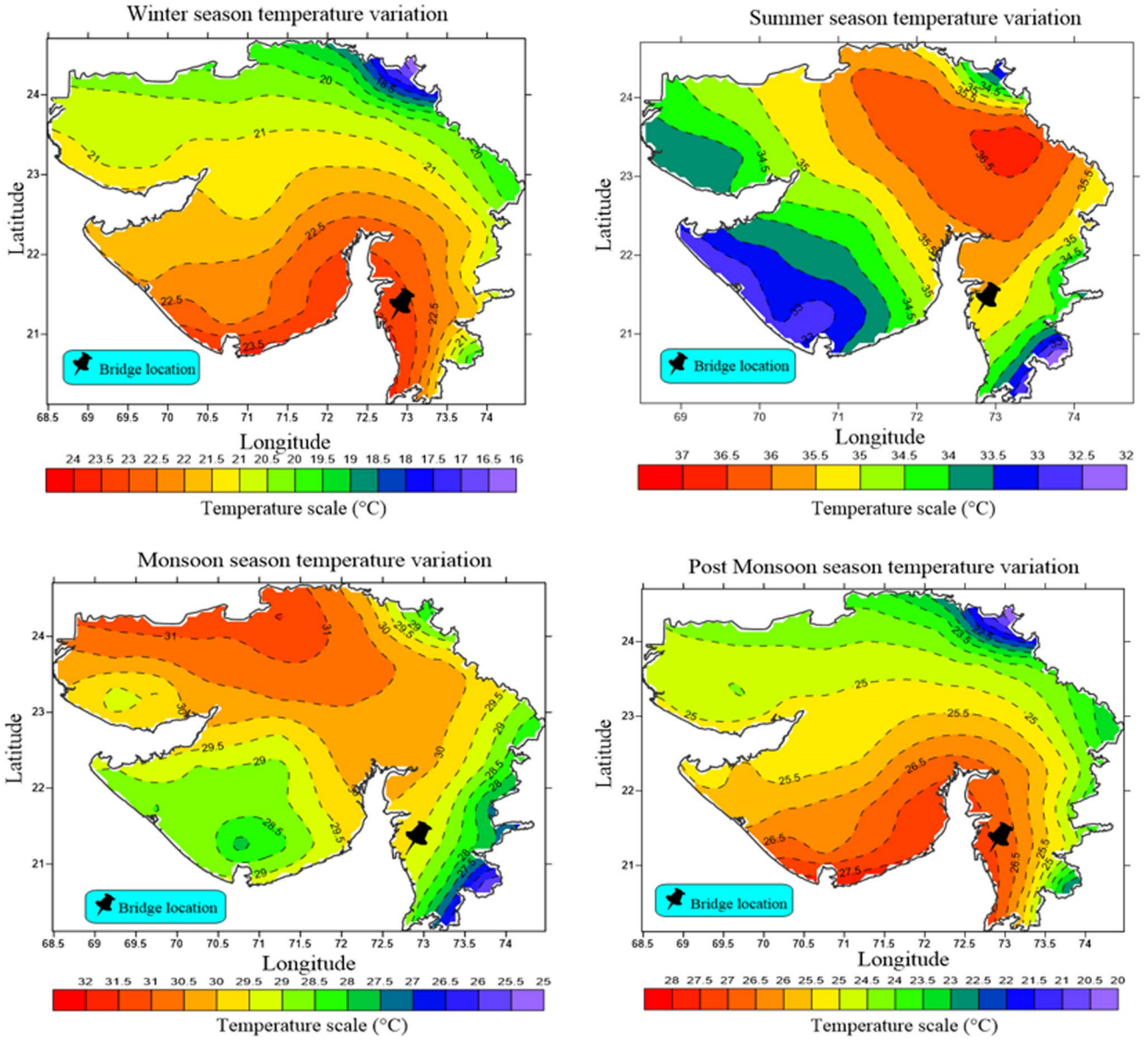

Fig. 13 Spatial distribution of temperature throughout the year in Gujarat (India) [NOAA]

$$\mathrm{Re}l(T) = \exp\left\{-\int_0^T \lambda_r(t)\left[1 - F_s\left(R_0 \times G(t)\right)\right]\mathrm{d}t\right\} \tag{21}$$

Thus, the probability of failure of the structure can be found out by:

$$p_f = 1 - \mathrm{Re}l(T) \tag{22}$$

Structural reliability assessment of bridge considering climatic factors

Bridge location and environmental factors

A highway RC bridge (known as Sardar Bridge) is selected to demonstrate the effect of temperature and humidity on time-dependent structural reliability. The selected bridge is taken from the earlier work of the authors [13] in which a framework to determine the serviceability and safety by implementation of time-dependent reliability was developed for the highway bridge under aggressive environment and under the action of time-dependent and time-independent loads. The chosen bridge is situated at Surat district of

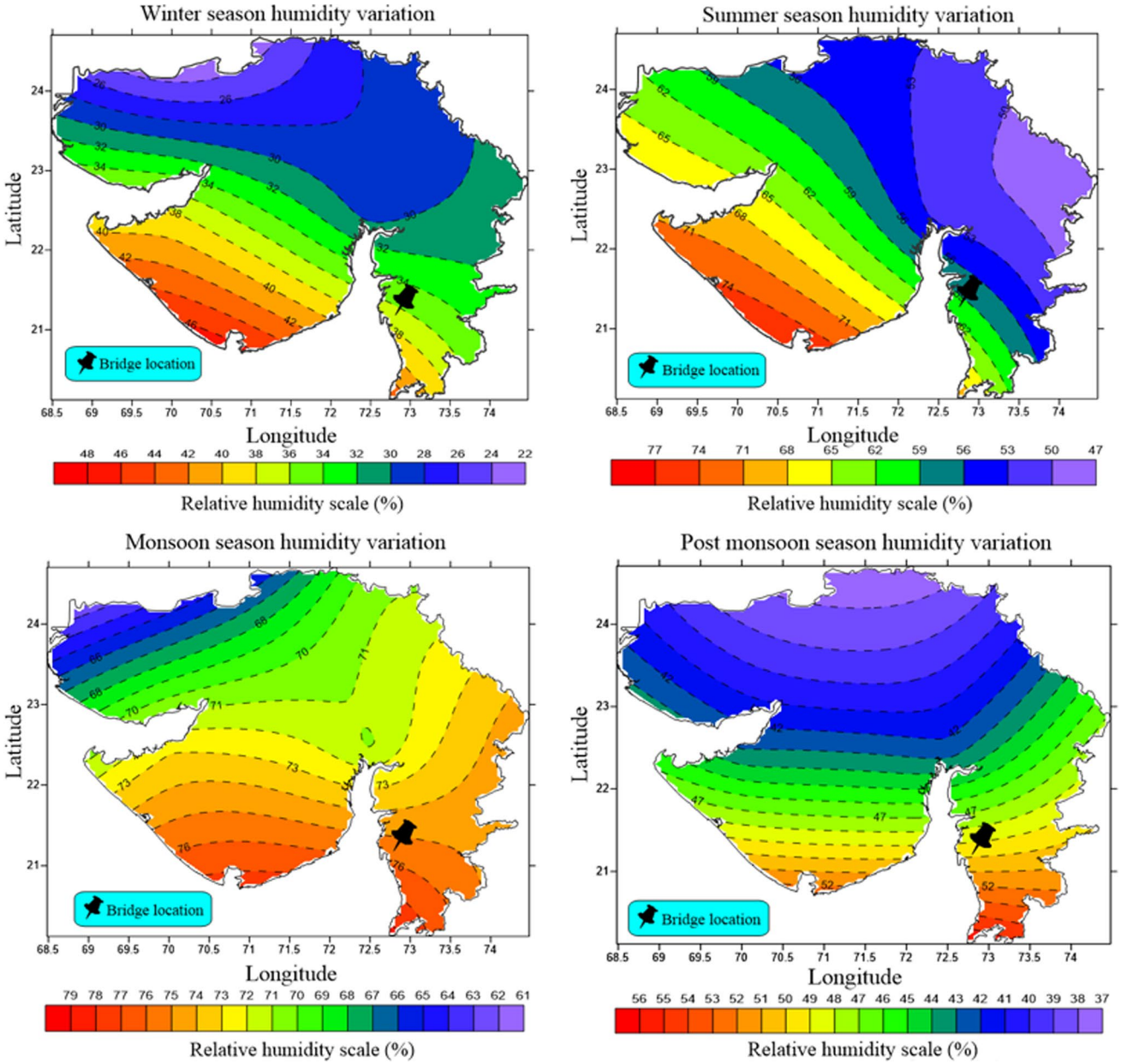

Fig. 14 Spatial distribution of relative humidity throughout the year in Gujarat (India) [NOAA]

Table 3 Average temperature and relative humidity at the bridge site in Gujarat

Season	Average Temperature (°C)	Average Relative Humidity (RH %)	Adjustment factors	
			f_T	f_{RH}
Winter	23.00	35.00	1.22	2.12E-11
Summer	35.00	60.00	2.09	0.93
Monsoon	29.50	75.50	1.69	1.00
Post-Monsoon	27.75	49.50	1.56	0.19

Gujarat (India). Built in year 1991 over Tapi river, this bridge serves as a major lifeline in transportation between two important cities (i.e. Athwa and Adajan). The bridge comprises of six number of girders, equally spaced, for every span of the bridge. The other technical details along with design parameters of the bridge are adopted from previous work of the authors [13] and are given in Table 2. Figure 11 displays the geographical site of the chosen bridge. Due to its close proximity with Arabian Sea, the bridge is exposed to chloride-contaminated marine environment. Therefore, keeping that in mind, three types of environmental aggressiveness are considered, i.e. Submerged, Tidal/Splash, and

Table 4 Parameters related to strength and loads [13]

Parameters	Moment	Nominal	Mean	Units	COV	Distribution
R_0	Initial resistance	4489.52	4711	kNm	0.14603	Normal
DL	Dead load	2864.76	3005	kNm	0.09985	Normal
LL1	Live load 1	2515.52	1677	kNm	0.22346	GEV
LL2	Live load 2	2155.71	1677	kNm	0.22346	GEV
LL3	Live load 3		$\mu_{L,3}(t) = \left(c_0 + c_1 \times t^{\alpha}\right)L_n$	kNm	0.22346	GEV

Atmospheric [15] to model the chloride ingress. The climate in Indian subcontinent keeps changing according to different season. Further, to consider the variation of in situ temperature and relative humidity, the year is divided into four seasons, i.e. Winter season (Dec–Feb); Summer season (Mar–May); Monsoon season (Jun–Sept); and Post-Monsoon (Oct–Nov) (Fig. 12). Figure 13 and Fig. 14 present the spatial and temporal variation of temperature and relative humidity to showcase the seasonal variation of both the parameters throughout Gujarat state. The datasets have been obtained from National Oceanic and Atmospheric Administration (NOAA) website. From Fig. 13 and 14, the temperature and relative humidity at the bridge site corresponding to different seasons is found and is given in Table 3.

Time-dependent reliability assessment with combined effect of non-stationarity in the loading method and in situ temperature and relative humidity conditions

Three models of live load were considered in order to exemplify the non-stationarity effect of live load. The mean values for live load model 1 (LL-1) and live load model 2 (LL-2) are time independent, while the mean value of live load 3 (LL-3) is kept time dependent and is represented as:

$$\mu_{L,3}(t) = \left(c_0 + c_1 \times t^{\alpha}\right)L_{\mathrm{n}} \tag{23}$$

where c_0 = initial intensity of mean load, c_1 = scale factor and α = shape factor.

The probabilistic models of load and resistance are given in Table 4. Please note that the initial resistance, dead load, and live load of the representative bridge considered in this study have been obtained from the earlier work of the authors [13]. The nominal structural resistance, R_n, is assessed as per design constraint of concrete structures [13]:

$$1.0R_{\mathrm{n}} = 1.5D_{\mathrm{n}} + 2.5L_{\mathrm{n}} \tag{24}$$

where R_{n} = Nominal resistance, D_{n} = Nominal dead load, L_{n} = Nominal live load.

For sake of convenience, it has been considered that $D_{\mathrm{n}} = L_{\mathrm{n}} = 1.0$. Therefore, the nominal structural resistance, R_{n} as per Eq. (23), is equal to 4.0.

Results and discussion

The time-dependent probability of failure F(t), for combined effect of various live load models, temperature and relative humidity conditions, and different chloride aggressive environments is computed using Eq. (21). Figure 14a, b and c demonstrates the effect of temperature and relative humidity on failure probability of the bridge when exposed to three different chloride-contaminated environment and under the action of live load model 1 (LL-1). It is clearly evident that the failure probability increases with an increase in time. Also, it is observed that the time-variant failure probability is sufficiently sensitive towards climatic factors like temperature and humidity. From Fig. 14a, it can be remarked that for submerged environment, deviation of temperature and humidity from reference values would lead to notable difference in failure probability of the structure. The failure probability calculated using reference condition of temperature of 20 °C and relative humidity of 75% is shown by a black coloured dotted line. It is observable that the failure probability is higher than the reference condition for summer season and monsoon season. This is due to the fact that during summer and monsoon season, the temperature and humidity levels are higher. The failure probability is less than the reference condition for post-monsoon and winter season, and the lowest during winter due to the fact that both temperature and humidity levels are low during these months. Therefore, the cruciality of considering the seasonal variation of temperature and humidity to determine the structural reliability is clearly noted and hence cannot be ignored. This further emphasizes the importance of considering temperature and humidity in modelling the chloride-induced corrosion process. Similar observations were also made in tidal/splash and atmospheric zone as shown in Fig. 14b, c.

When the corrosion degradation due to chloride ingress is accompanied by the deterioration caused due to loads acting on the bridge structure, the combined effect on the corrosion mechanism is predominant. The degradation of the structural resistance is considered to be linearly varying for all the live load models (Fig. 15). The failure probability is plotted for three different environmental aggressiveness along with change of seasons and different live load models as shown in Fig. 16a, b and c. From Fig. 16a, it is observed that for submerged zone, the failure probability is greatest

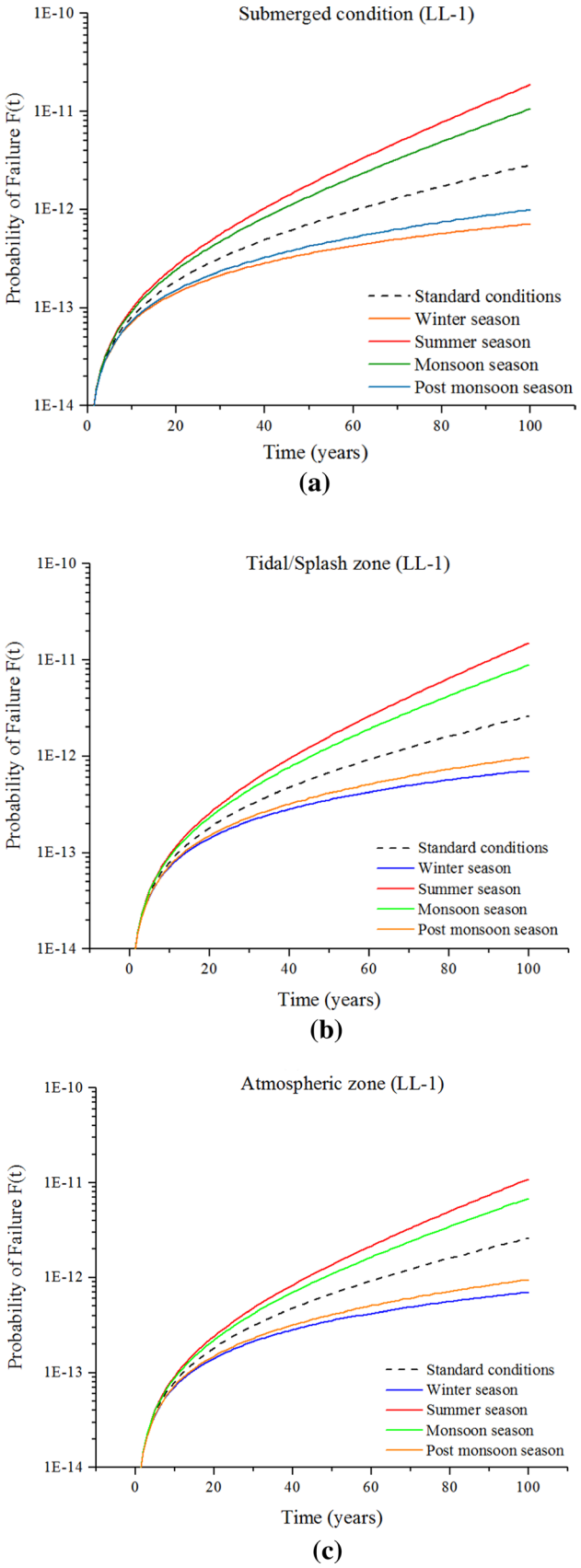

Fig. 15 Time-dependent failure probability of the RC bridge for live load model 1 (LL1) under various environmental aggressiveness and seasonal variations (**a**) Submerged zone (**b**) Tidal/splash zone (**c**) Atmospheric zone

corresponding to live load case LL2 followed by LL3 and LL1 load cases until a period of 40 years, after which the LL3 case surpasses the LL2 case and exhibits the highest failure probability. The probability of failure corresponding to LL3 rises in a quick pace owing to an increase in the mean load intensity of LL3 as compared to LL2 with respect to time. Thus, it can be concluded that the service life of the structure also plays a vital role for LL3 case in estimation of probability of failure of the structure. The effect of seasonal change is also shown in Fig. 16a, b and c where the summer season exhibits the highest failure probability followed by monsoon and post-monsoon season, while it is the lowest for winter season for all the three live load models. Thus, temperature and relative humidity together with applied live loads exerts a strong influence in the determination of failure probability of a structure.

The collective effect of type of exposure environment together with seasonal change can be observed in Fig. 17, which demonstrates the variation of probability of failure considering live load case 1 for different exposure environments and varying climatic parameters. It is seen from the figure that for all the three environmental aggressiveness, the time-variant failure probability of the bridge structure is closely identical. This happens essentially due to small variations in the resistance degradation function, G(t), which in turn leads to lesser variations in the rate parameter, k for each exposure condition resulting in a lesser reduction in the time-variant structural resistance, R(t). It is observed that the temperature and relative humidity variation as per seasons plays a crucial role in determining the failure probability. As seen from figure, the failure probability in summer season is the highest among all irrespective of environmental exposure. For instance, the failure probability of tidal and atmospheric zone in summer is greater than the failure probability of submerged zone in winter, post-monsoon, and monsoon season. Therefore, it is seen that even in less aggressive environment, the failure probability can exceed when exposed to greater temperature and relative humidity. Thus, it clearly evident that how change of season can largely vary the failure probability of structure.

Until now, the time-variant live load model (LL-3) is considered to be linearly varying, i.e. considering shape factor $\alpha = 1$. By considering different shape factors of live load model LL-3, four different live load models are considered viz. linear model ($\alpha = 1$), square root model ($\alpha = 0.5$), parabolic model ($\alpha = 2$), and cubic model ($\alpha = 3$). Accordingly, Fig. 18 shows the calculated failure probability of the bridge under submerged condition by taking different time-variant

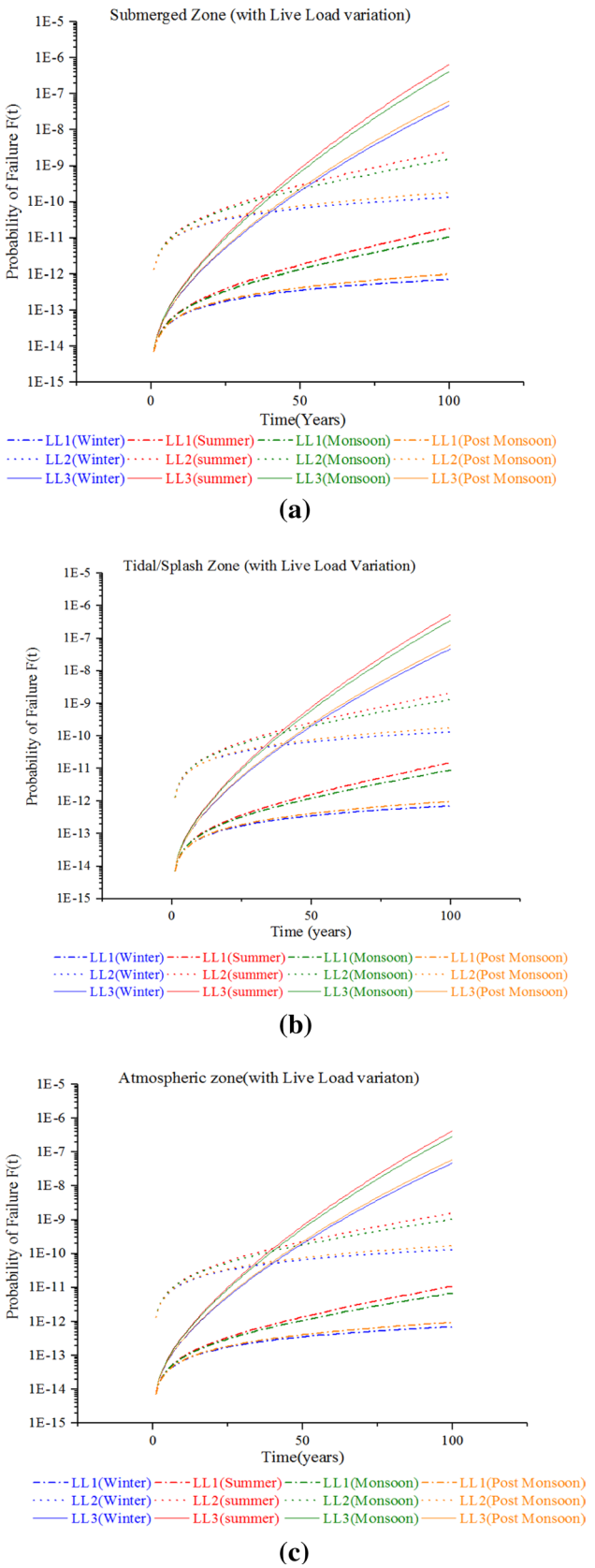

Fig. 16 Influence of various live load models on the time-variant failure probability of the RC bridge under various aggressive environment and variation of seasonal parameters (**a**) Submerged zone (**b**) Tidal/splash zone (**c**) Atmospheric zone

live load models. From the figure, it has been observed for a higher value of the shape parameter that the failure probability of the representative bridge increases significantly. Also, it has been observed that there is a prompt increase in the failure probability of the parabolic model as compared to square root and linear model. The parabolic model and cubic model has a failure probability of 100% after a service life period of 32 years and 13 years, respectively. The output of both the parabolic and cubic model is well beyond the conservative estimate of the actual degradation process, while square root model underestimates the degradation process. Therefore, for making a reliable estimate of the failure probability under time-variant loading conditions, the linear model may be considered as the most suitable one.

Conclusions

By capturing the influence of temperature and relative humidity in the chloride-induced corrosion degradation process, the presented work has proposed a novel approach for estimating the reliability of RC bridges located in marine environments and subjected to multiple hazards like chloride-induced corrosion and live loads acting on the structure. In addition, the paper focusses on the variability of temperature and relative humidity of a region with respect to changing seasons. The model presented in the paper is able to take into account the influence of in situ temperature and humidity conditions on corrosion degradation process while calculating the reliability of a structure. Corresponding to four seasons in India, i.e. winter, summer, monsoon and post-monsoon, the effect of variation of both temperature and relative humidity with respect to seasons is captured by introducing adjustment factors for temperature and relative humidity to calculate the modified corrosion rate for the corrosion degradation process. It is observed that with the gradual increase in temperature, the rate of degradation also increases. This is due to the fact that higher temperature accelerates the ingress of chloride into concrete, therefore the adjustment factor of temperature is found to be linearly increasing with rising temperature. While the relative humidity may either increase or decrease the degradation rate based on the moisture content.

As an application, the advanced corrosion rate model was applied on a representative T-girder bridge (named Sardar Bridge) subjected to chloride ingress and action of time-variant and time-invariant loading conditions acting on the bridge, also taking into account the in situ climatic condition

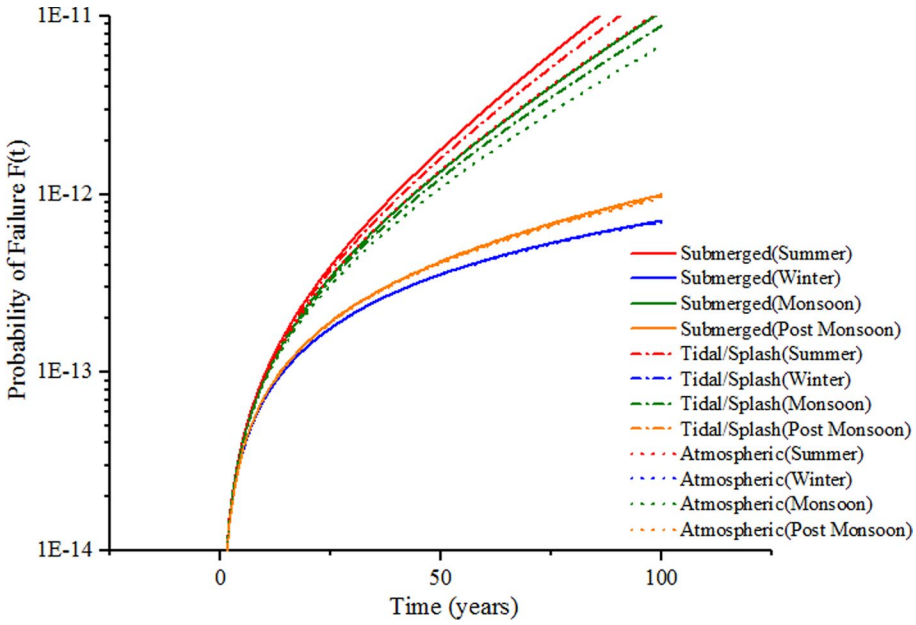

Fig. 17 Comparison among failure probability of different environmental aggressiveness in different seasons

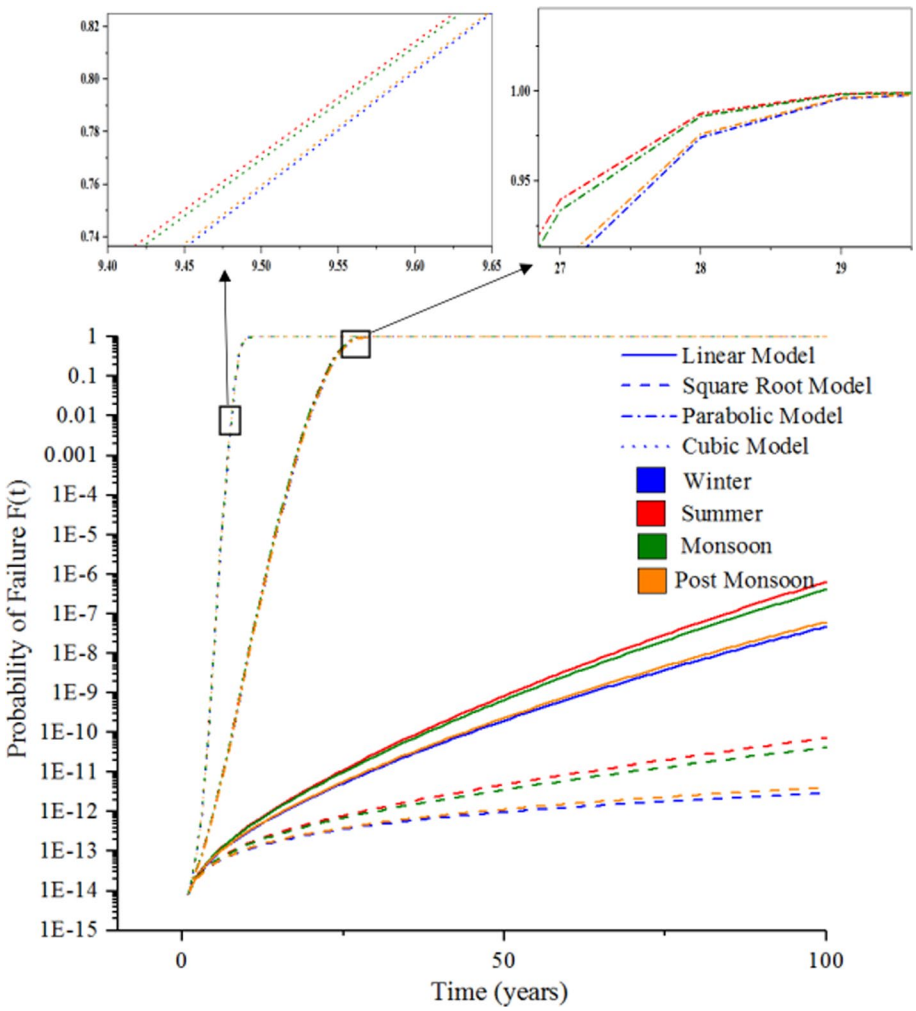

Fig. 18 Influence of shape factor of LL3 on the probability of failure in submerged zone

to calculate the structural reliability of the structure. The reliability analysis carried out on the structure indicates the effect of type of environmental exposure, live load conditions, and climatic factors on the failure probability of the structure. The three live load models taken into consideration indicates that the failure probability of structures subjected to live load 3(LL-3) is higher as compared to live load model LL-1 and LL-2. Therefore, it can be concluded that the time-variant live load model would have a higher influence on the failure probability than the time-invariant live load models. Furthermore, a significant rapid increase in failure probability is observed in case of live load model 3(LL-3) on taking higher values of shape parameter.

The effect of climatic condition like temperature and relative humidity was also seen in the reliability analysis. The effect of seasonal variation of temperature and relative humidity at the bridge site in the failure probability of the structure was apparent from the study. From Fig. 10a, b and c, it is evident that how considering variation of seasonal parameters the probability of failure varies from the reference condition. It is observed that the failure probability is the highest in summer season, followed by monsoon season. This must be attributed to the fact that in both the seasons, the temperature and relative humidity values are high, whereas the failure probability is the lowest for winter season and post-monsoon season due to low temperature and relative humidity. Thus, this highlights the importance of considering the climatic factors like temperature and relative humidity in reliability analysis of RC bridges exposed to chloride-induced deterioration.

Declarations

Conflict of interest On behalf of all authors, the corresponding author states that there is no conflict of interest.

References

1. Andrade C, Castillo A (2003) Evolution of reinforcement corrosion due to climatic variations. Mater Corros 54(6):379–386. https://doi.org/10.1002/maco.200390087
2. Bastidas-Arteaga E, Sánchez-Silva M, Chateauneuf A, Ribas SM (2008) Coupled reliability model of biodeterioration, chloride ingress and cracking for reinforced concrete structures. Struct Safety 30(2):110–129
3. Bastidas-Arteaga E, Bressolette P, Chateauneuf A, Sánchez-Silva M (2009) Probabilistic lifetime assessment of RC structures under coupled corrosion-fatigue deterioration processes. Struct Safety 31(1):84–96
4. Bastidas-Arteaga E, Chateauneuf A, Sánchez-Silva M, Bressolette P, Schoefs F (2010) Influence of weather and global warming in chloride ingress into concrete: a stochastic approach. Struct Saf 32(4):238–249. https://doi.org/10.1016/j.strusafe.2010.03.002
5. Bastidas-Arteaga E, Schoefs F, Stewart MG, Wang X (2013) Influence of global warming on durability of corroding RC structures: a probabilistic approach. Eng Struct 51(Jun):259–266. https://doi.org/10.1016/j.engstruct.2013.01.006
6. Borah MM, Dey A, Sil A (2020) Service life assessment of chloride affected bridge located in coastal region of India considering variation in the inherent structural parameters. Structures 23:191–203
7. Çadraku HS, Jagxhiu B (2020) Sustainability and functionality of railway network and its connecting facilities in Kosovo. J Hum Earth Future 1(3):112–121
8. Chauhan A, Sharma UK (2019) Influence of temperature and relative humidity variations on non-uniform corrosion of reinforced concrete. Structures 19:296–308. https://doi.org/10.1016/j.istruc.2019.01.016
9. Choe DE, Gardoni P, Rosowsky D, Haukaas T (2009) Seismic fragility estimates for reinforced concrete bridges subject to corrosion. Struct Saf 31(4):275–283. https://doi.org/10.1016/j.strusafe.2008.10.001.
10. Dacuan CN, Abellana VY, Canseco HAR (2021) Assessment and evaluation of blended cement using bamboo leaf ash BLASH against corrosion. Civ Eng J 7(6):1015–1035
11. de Medeiros-Junior RA, de Lima MG, de Medeiros MHF (2015) Service life of concrete structures considering the effects of temperature and relative humidity on chloride transport. Environ Dev Sustain 17:1103–1119. https://doi.org/10.1007/s10668-014-9592-z
12. Dey A, Sil A (2021) Advanced corrosion-rate model for comprehensive seismic fragility assessment of chloride affected RC bridges located in the coastal region of india. Structures 34:947–963. https://doi.org/10.1016/j.istruc.2021.08.045
13. Dey A, Miyani G, Sil A (2019) Reliability assessment of reinforced concrete (RC) bridges due to service loading. Innov Infrastruct Solut. https://doi.org/10.1007/s41062-018-0194-8
14. Duprat F (2007) Reliability of RC beams under chloride-ingress. Constr Build Mater 21(8):1605–1616. https://doi.org/10.1016/j.conbuildmat.2006.08.002
15. Duracrete (2000) Probabilistic performance-based durability design of concrete structures. Final Tech Rep. Brussels, Belgium: European Union
16. Enright MP, Frangopol DM (1998) Probabilistic analysis of resistance degradation of reinforced concrete bridge beams under corrosion. Eng Struct 20(11):960–971
17. Ghosh J, Padgett JE (2012) Impact of multiple component deterio- ration and exposure conditions on seismic vulnerability of concrete bridges. Earthquake Struct 3(5):649–673. https://doi.org/10.12989/eas.2012.3.5.649
18. Guo Y, Trejo D, Yim S (2015) New model for estimating the time-variant seismic performance of corroding RC bridge columns. J Struct Eng 141(6):04014158. https://doi.org/10.1061/(ASCE)ST.1943-541X.0001145
19. Hassan EJ, Bressolette P, Chateauneuf A, Tawil KE (2010) Reliability-based assessment of the effect of climatic conditions on the corrosion of RC structures subject to chloride ingress. Eng Struct 32(10):3279–3287. https://doi.org/10.1016/j.engstruct.2010.07.001
20. https://psl.noaa.gov/cgi-bin/data/testdap/timeseries.pl
21. Hussain RR, Tetsuya I (2010) Novel approach towards calculation of averaged activation energy based on arrhenius plot for modeling of the effect of temperature on chloride induced corrosion of steel in concrete. J ASTM Int 7(5):1–8
22. Hussain RR (2010) Enhanced classical tafel diagram model for corrosion of steel in chloride contaminated concrete and the nonlinear experimental effect of temperature. Int J Concr Struct Mater 4(2):71–75
23. Hussain RR (2011) Effect of moisture variation on oxygen consumption rate of corroding steel in chloride contaminated concrete. Cem Concr Compos 33(1):154–161

24. Liu T, Weyers RW (1998) Modelling the dynamic corrosion process in chloride contaminated concrete structures. Cem Concr Res 28(3):365–379. https://doi.org/10.1016/S0008-8846(98)00259-2
25. MacGregor JG, Mirza SA, Ellingwood B (1983) Statistical analysis of resistance of reinforced and prestressed concrete members. J Am Concr Inst 80(3):167–176
26. Madlangbayan MS, Diola CNB, Tapia AKG, Peralta MM, Peralta EK, Almeda RA, Bayhon MAL, Sundo MB (2021) Corrosion inhibition of sodium silicate with nanosilica as coating in pre-corroded steel. Civ Eng J 7(11):1806–1816. https://doi.org/10.28991/cej-2021-03091761
27. Marsh PS, Frangopol DM (2008) Reinforced concrete bridge deck reliability model incorporating temporal and spatial variations of probabilistic corrosion rate sensor data. Reliab Eng Syst Saf 93(3):394–409
28. Martin-Perez B, Pantazopoulou SJ, Thomas MDA (2001) Numerical solution of mass transport equations in concrete structures. Comput Struct 79(13):1251–1264. https://doi.org/10.1016/S0045-7949(01)00018-9
29. Nilsson L-O (2001) Prediction models for chloride ingress and corrosion initiation in concrete structures. In: Nilsson LO (ed) P-01:6 Chalmers University of Technology
30. Parrott LJ (1991) Factors influencing relative humidity in concrete. Mag Concr Res 43(154):45–52
31. Peng L, Stewart MG (2014) Spatial time-dependent reliability analysis of corrosion damage to RC structures with climate change. Mag Concr Res 66(22):1154–1169. https://doi.org/10.1680/macr.14.00098
32. Stewart MG, Mullard JA (2007) Spatial time-dependent reliability analysis of corrosion damage and the timing of first repair for RC structures. Eng Struct 29:1457–1464. https://doi.org/10.1016/j.engstruct.2006.09.004
33. Stewart MG, Rosowsky DV (1998) Structural safety and serviceability of concrete bridges subject to corrosion. J Infrastruct Syst 4(4):146–155
34. Stewart MG, Rosowsky DV (1998) Time-dependent reliability of deteriorating reinforced concrete bridge decks. Struct Saf 20(1):91–109
35. Stewart MG, Vu KAT (2000) Structural reliability of concrete bridges including improved chloride-induced corrosion models. Struct Saf 22(4):313–333. https://doi.org/10.1016/S0167-4730(00)00018-7
36. Stewart MG (2004) Spatial variability of pitting corrosion and its influence on structural fragility and reliability of RC beams in flexure. Struct Safety 26(4):453–470
37. Stewart MG, Wang X, Nguyen MN (2011) Climate change impact and risks of concrete infrastructure deterioration. Eng Struct 33(4):1326–1337. https://doi.org/10.1016/j.engstruct.2011.01.010
38. Thomas MDA, Bentz D (2018) Life 365 computer program for predicting the service life and life-cycle costs of reinforced concrete structures exposed to chlorides. User Manual (version 2.2.3)
39. VillagránZaccardi YA, Bértora A, Di Maio AA (2013) Temperature and humidity influences on the on-site active marine corrosion of reinforced concrete elements. Mater Struct 46:1527–1535. https://doi.org/10.1617/s11527-012-9994-z
40. Wang X, Stewart MG, Nguyen M (2012) Impact of climate change on corrosion and damage to concrete infrastructure in australia. Clim Chang 110(3–4):941–957. https://doi.org/10.1007/s10584-011-0124-7
41. Yu B, Liu J, Li B (2017) Improved numerical model for steel reinforcement corrosion in concrete considering influences of temperature and relative humidity. Constr Build Mater 142:175–186. https://doi.org/10.1016/j.conbuildmat.2017.03.045